Final Report: Susan Deutscher
Report/Product Number: DOE-MU-0002121
DOE Award/Contract Number: SC0002121
Recipient/Contractor Organization: The Curators of the University of Missouri, Office of Sponsored Programs, University of Missouri, 310 Jesse Hall, Columbia, MO 65211-1230

**Students trained:** Benjamin Larimer (09/01/2010-12/31/2010 & 09/01/2011-06/14/2013)
**Post-Doc:** Mark Palmier (12/01/2009-12/31/2011) Xiuli Zhang (07/01/2010-04/30/2011)

**Others on grant at some point:**
Terry Carmack (03/01/2011-07/31/2011 and 08/01/2010-02/28/2010)
Cathy Cutler 10/01/2009-09/30/2011
Susan Deutscher10/01/2009-5/31/2013
Fabio Gallazzi10/01/2009-6/30/2012
Jessica Newton04/01/2011-6/30/2011
Tom Quinn10/01/2009-08/31/2011
Lisa Watkinson07/01/2010-02/28/2011
Lisa Watkinson03/01/2011-07/31/2011

**Publications: None**

**Specific Aims:**
**1. Engineer galectin-3 (gal-3) and carbohydrate Thomsen-Friedenrich (TF)-binding peptide cyclotide conjugates.**

We first determined key residues for gal-3 binding peptide G3-C12 to bind the lectin gal-3. Alanine scanning mutants were constructed (Table 1).

**Table 1. Alanine Scanning m Mutants of G3-C12 peptide.**

| Code | Sequence |
|---|---|
| G3-C12 | A N T P C G P Y T H D C P V K R |
| Ala1Ser | **S** N T P C G P Y T H D C P V K R |
| Asn2Ala | A **A** T P C G P Y T H D C P V K R |
| Thr3Ala | A N **A** P C G P Y T H D C P V K R |
| Pro4Ala | A N T **A** C G P Y T H D C P V K R |
| Cys5Ala | A N T P **A** G P Y T H D C P V K R |
| Gly6Ala | A N T P C **A** P Y T H D C P V K R |
| Pro7Ala | A N T P C G **A** Y T H D C P V K R |
| Try8Ala | A N T P C G P **A** T H D C P V K R |
| Thr9Ala | A N T P C G P Y **A** H D C P V K R |
| His10Ala | A N T P C G P Y T **A** D C P V K R |
| Asp11Ala | A N T P C G P Y T H **A** C P V K R |
| Cys12Ala | A N T P C G P Y T H D **A** P V K R |
| Pro13Ala | A N T P C G P Y T H D C **A** V K R |
| Val14Ala | A N T P C G P Y T H D C P **A** K R |
| Lys15Ala | A N T P C G P Y T H D C P V **A** R |
| Arg16Ala | A N T P C G P Y T H D C P V K **A** |
| Cys5&12Ala | A N T P **A** G P Y T H D **A** P V K R |
| Negative Control | **N T P A D** G P Y T H D **A** P V K R |

An enzyme linked immunosorbant assay (ELISA) was performed with the peptides to purified gal-3 (Figure 1).

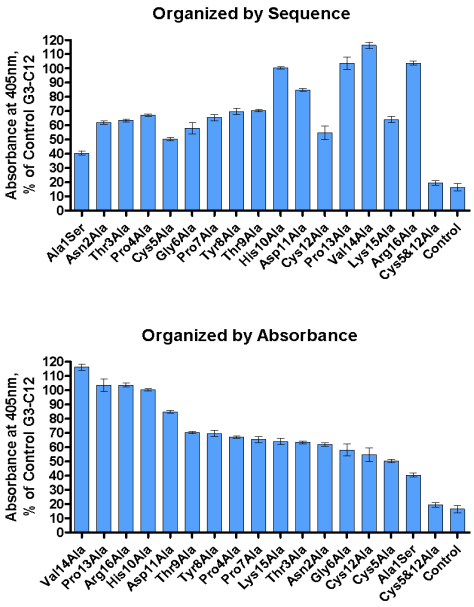


**Figure 1. ELISA of Gal-3 Ala Scanning Mutants.**

The ability of the mutants to bind cells expressing gal-3 (MDA-MB-435) and cells not expressing gal-3 (PC3) was examined next by confocal microscopy (Figure 2).

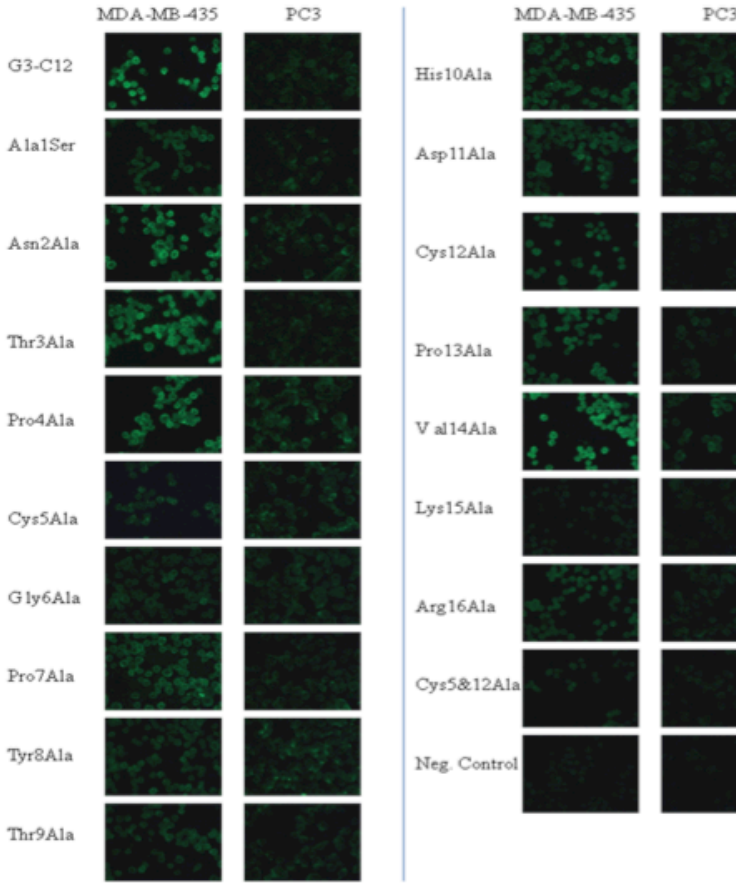


**Figure 2. Confocal Microscopy of Binding of G3-C12 Mutants to Cell Lines.**

These studies identified residues 1-5, and 12 as important residues in binding. In order to determine the minimal binding motif of G3-C12, A series of Gal-3-targeting peptide variants of G3-C12 were synthesized (Table 2) and analyzed for binding using ELISA. Cyc-ts10 and Cyc-ts11 retained binding to gal-3 but had reduced affinity from 72nM to ~ 150 nM (Fig 3).

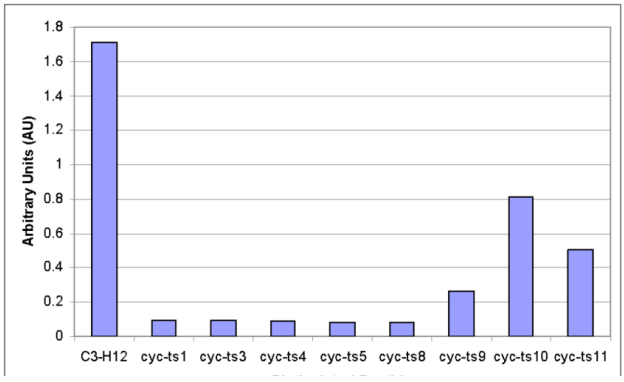


**Table 3. G3-C12 Variants**

| Code | Sequence |
|---|---|
| G3-C12 | A N T P C G P Y T H D C P V K R |
| cyc-ts1 | A G P Y T H D |
| cyc-ts3 | A P **S** G P Y T H D |
| cyc-ts4 | A G P Y T H D **S** P |
| cyc-ts5 | A **P** G P T F L D |
| cyc-ts8 | A **A** G P Y T H D **A** |
| cyc-ts9 | A **A** G P Y T H D C |
| cyc-ts10 | A C G P Y T H D **A** |
| cyc-ts11 | A C G P Y T H D C |

**Figure 3. Binding of Gal-3-avid Peptides.** ELISA plates were coated with 0.5 µg of gal-3 protein. A solution of 10 µM of biotinylated peptide was then incubated with the protein for 1 h at room temperature. Following incubation with streptavidin-HRP conjugate, the plate was developed and absorbance at 405 nm read.

We chose to graft the gal-3-avid (G3-c12, ts10) and TF peptide (TF minimum binding motif WYAWSP) into the kalataB1 cyclotide. Kalata B1 is a good choice among cyclotides to use as a scaffold. While displaying the typical knotting stability characteristics it has also been shown to resist cellular internalization, remaining on the targeted cell surface. The mature kalata B1 sequence is CGETCVGGTCNTPGCTCSWPVCTRNGLPV. We first engineered G3-C12 (ANTPCGPYTHDCPVKR) in kalata B1. Using evolutionary trace analysis, we predicted the most promising site for C12 insertion into kalata B1. Shown is a summary depiction of the evolutionary trace results (Figure 4). The residues comprising kalata B1 are color coded to illustrate their predicted importance to the structure/function.

The bar below is the color key defining explaining the sequence map. Dark grey, black, reds and yellow colored residues would indicate they are critical for maintaining the structure of their protein/peptide. The residues comprising the sequence string T23 R24 N25 G26 L27 P28 V29 are predicted to have a minimal effect on the knottin structure and therefore seen as the most promising sites of substitution. Not surprisingly, this site is within loop 6, which has been previously reported to be the best site for targeting peptide insertion.

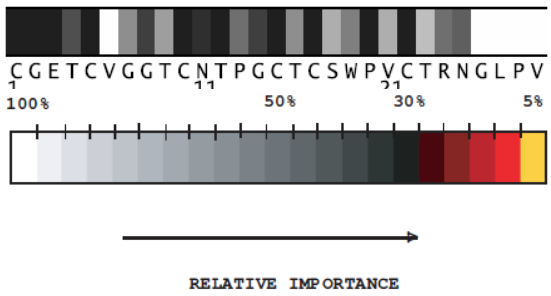


**Figure 4. Evolutionary Trace Analysis.** Using evolutionary trace analysis, we predicted the most promising site for C12 insertion into kalata B1.

Guided by the results of the bioinformatic analysis, we designed the sequences shown below: Figure 5 is a comparison of the disulfide bond maps of native Kalata B1 and the three and four-disulfide models.

**Figure 5. Disulfide Maps of Kalata B2 and Mutations Containing The Galectin-3 Avid Peptide Sequence**

A
Kalata B1

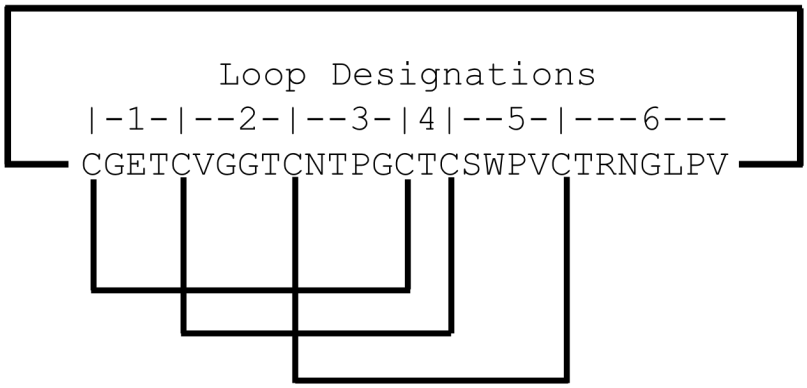


B

Cyclic Peptide Design Strategy (A); Four-disulfides

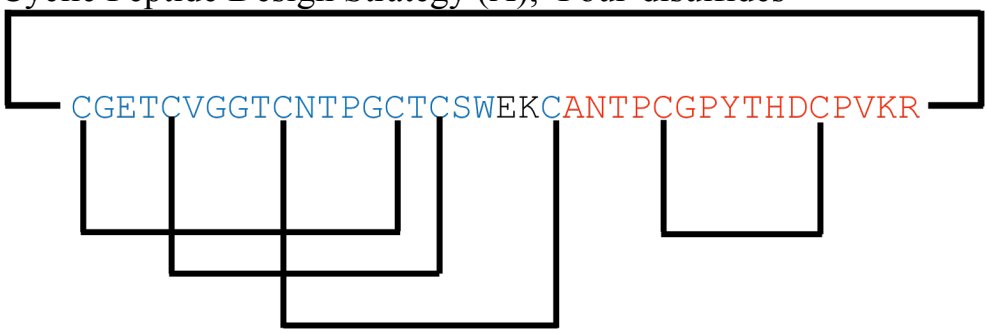


C

Cyclic Peptide Design Strategy (B); Three Disulfides

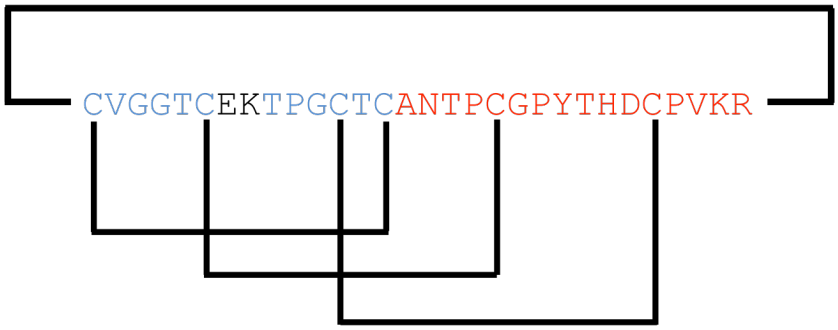


Figure 6 illustrates the comparative structures of both models as predicted by the Knotter 1D3D predictive folding algorithm as compared to the native Kalata B1 that was solved by NMR. The lack of secondary structure illustration is due to the nature of the output data from Knotter 1D3D.

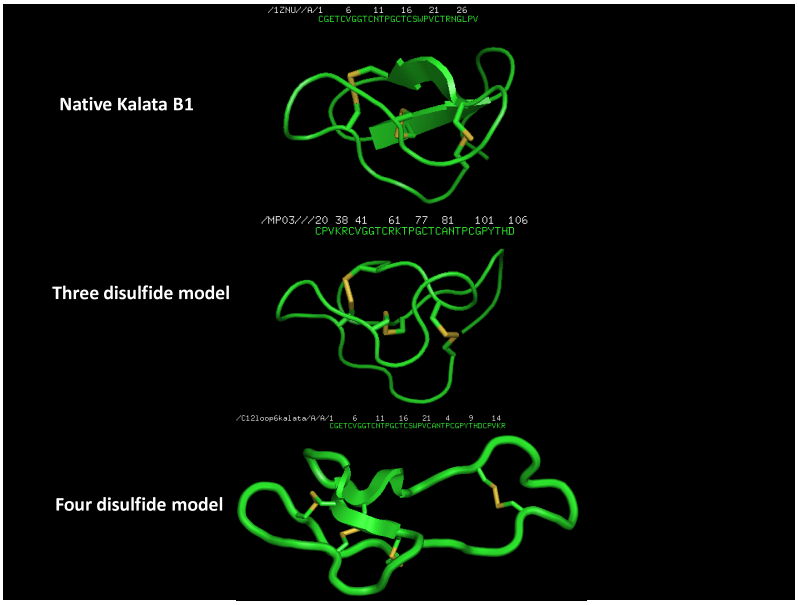


**Figure 6. Comparison of Structures for Kalata B1 compared to the Three and Four-disulfide Models**

The structural alignment of the structures is shown in Figure 7.

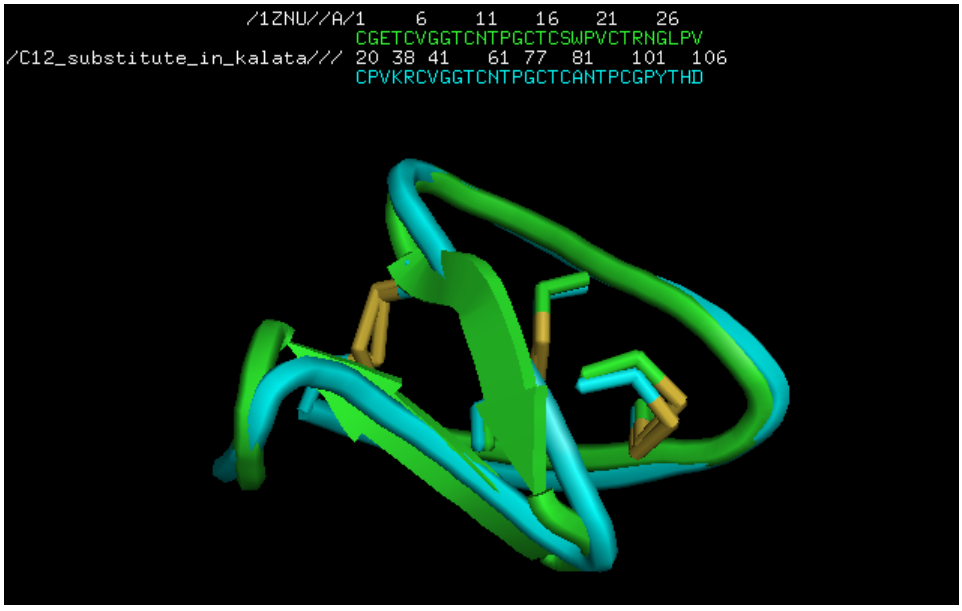


**Figure 7. Structural alignment of the three-disulfide model with native Kalata B1 shows a close match.**

Not surprisingly, the close alignment of both native Kalata B1 (Green) and the three-disulfide model (Light Blue) reflects the close match in their respective disulfide maps. Care should be taken in noting that the structure prediction for the 3-disulfide model was determined by Knotter 1D3D. This program uses primary sequence comparisons to Kalata B1 and similar cyclotide knottins in order to predict the final folding structure. The alignment of cysteines in the three-

disulfide model was made to be as close as possible to native Kalata B1 while not perturbing the inserted gal-3 binding sequence.

We modeled the kalata B1-G3-C12 hybrid molecule by removing the residues TRNGLPV from the NMR solution structure, 1ZNU. We then inserted G3-C12 sequence in this opened site. Using SYBYL computational routines, we ran a bond stress minimization followed by a simulated annealing computation. The final structure is shown in Figure 8.

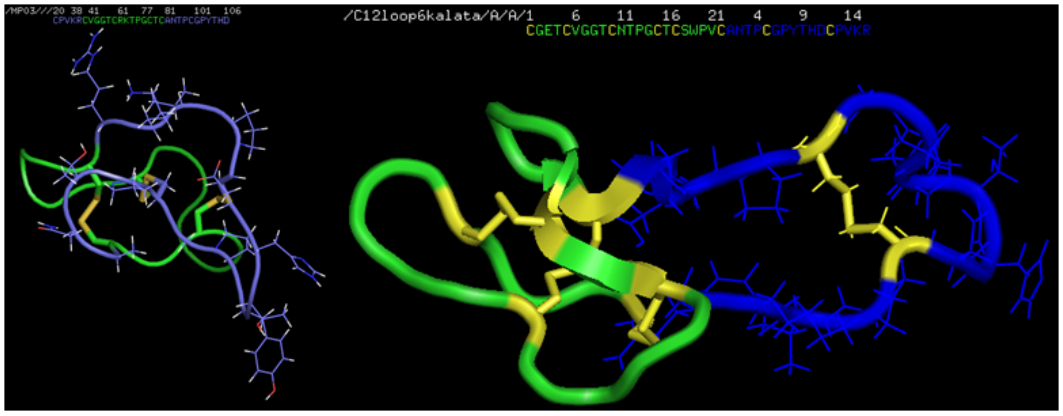


**Figure 8. Kalata B1-G3-C12 Hybrid.** We modeled the kalata B1-G3-C12 hybrid molecule using SYBYL by removing the residues TRNGLPV from the NMR solution structure, 1ZNU.

We also engineered kalata B1-cyc-ts-10 hybrid molecule using a similar strategy.

A series of refolding experiments were done to find good oxidative conditions that maximized solubility throughout the refolding period. Reverse phase HPLC, using a linear acetonitrile gradient, was used to gauge the extent and quality of refolding in this set of experiments. We compared 4°C to room temperature and found room temperature refolding was better. Adding organic solvent enhanced the solubility during refolding. Solvents we tested were acetonitrile, isopropanol, ethanol, methanol and DMSO and DMF. Of these isopropanol proved the best. We tested refolding at pH ranges from 7.0 to 9.0. We found pH 8.2 to 8.5 to be the optimized range. We tested whether glutathione or cysteine were better agents to enhance disulfide formation. We found 5 mM glutathione and 0.1 mM oxidized glutathione to be the best redox promoters in our hands. To find these more optimized conditions we ran a matrix of refolding conditions testing each variable with every other variable, appraising refolding by HPLC analysis. Overall, at room temperature using 50% isopropanol, 5 mM glutathione, 0.1 mM oxidized glutathione, in 0.1 M ammonium bicarbonate, pH 8.2 gave the best refolding results of our variable matrix combinations.

Using these conditions the typical refolding pattern by HPLC is shown below (Figure 9). HPLC was monitored at 280 nm. The blue trace is the refolding reaction after 3 days, the purple trace is the denatured starting material prior to refolding. Notice the sharpest most abundant refolded peak is later eluting in the acetonitrile gradient than the denatured starting material. This phenomenon is also seen with synthesized native kalata B1. Sharper peaks indicate more homogeneous refolding species.

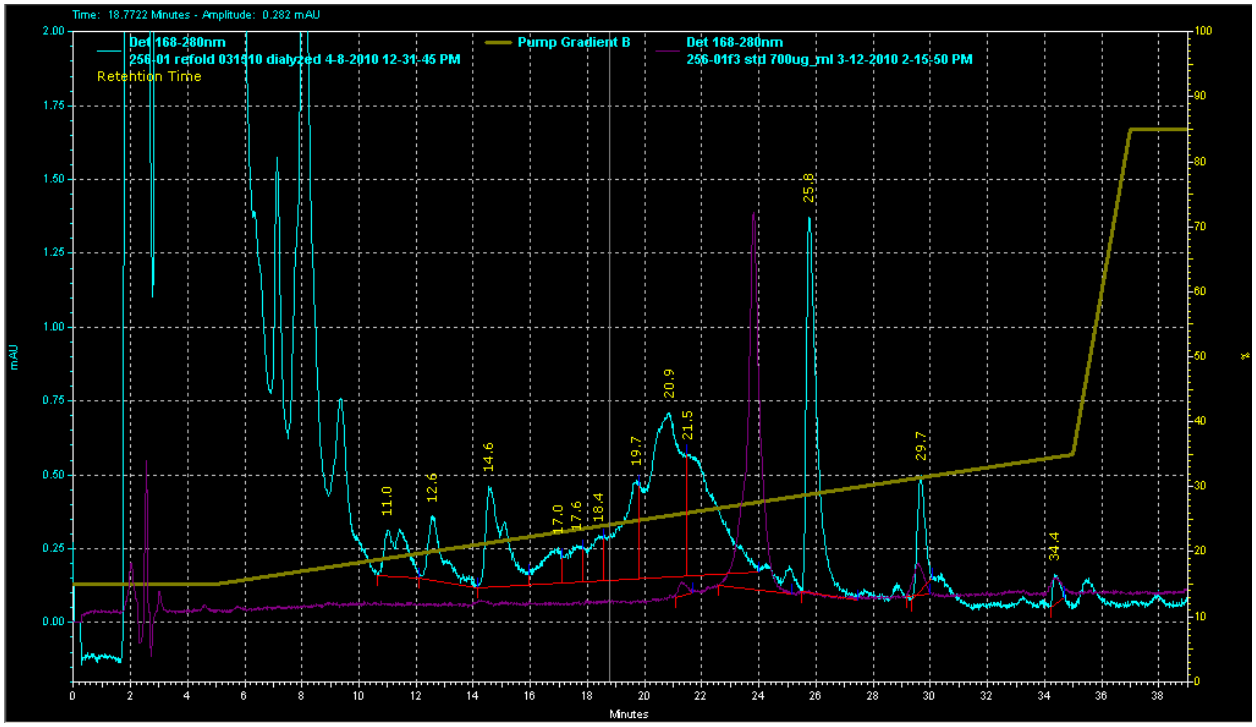


**Figure 9. Refolding Pattern of Cyclotide-G3-C12.**

After purification by HPLC the final folded product is shown in the reverse phase HPLC trace shown below. The green trace is the purified refolded material and the blue trace is the denatured starting material (Figure 10).

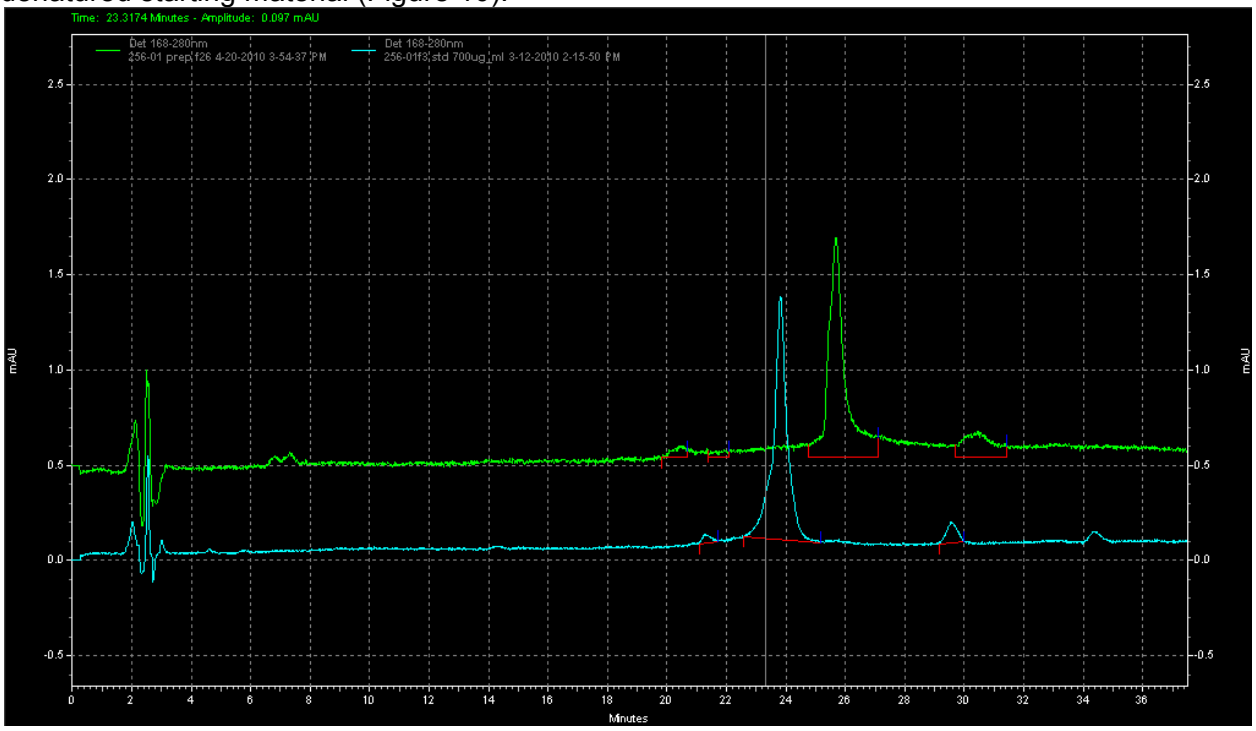


**Figure 10. Purified Folded G3-C12 Cyclotide.** The purified refolded material was analyzed by MALDI-TOF. The molecular weight was determined to be that of the starting material -8AMU, indicating the loss of 8 hydrogens and formation of 4 disulfide bonds. The denatured peptide starting material gave a major component $[M+H]^+$ of 3946 AMU. The refolded peptide gave a result of 3938 AMU.

We next determined if the folded cyclotides could bind cells expressing gal-3 (Figure 11). AS shown the G3-12 epitope in the cyclotide bound well to gal-3 expressing cells (MDA-MB-435) but no to gal-negative PC3 cells.

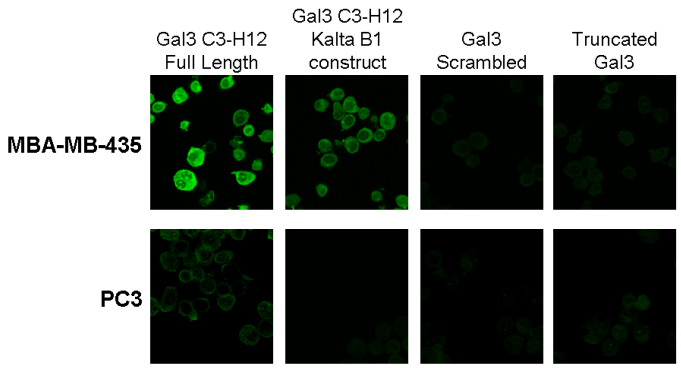


**Figure 11. Confocal Microscopy Showing Cyclotide-G3-C12 construct Binding to Gal-3-expressing Cells.**

## 2. Radiolabel cyclotides with $^{68}$Ga ($^{99m}$Tc, or $^{111}$In) and characterize radiolabeled conjugates.

The cyclotides were synthesized with both a biotin and DOTA and NOTA Chelate. Compound stability was tested in vitro by incubating $^{111}$In-DOTA radiolabeled test compounds in mouse serum for 14 h. Radiolabeling was performed at 60° for 1 h. Each was characterized by reversed phase HPLC analysis. Each chromatogram traces the simultaneous measurements of radioactivity on top and absorbance at 280 nm on the bottom. At 14 h, there is essentially no early eluting compound. The bulk of the radioactivity is in a broad late eluting peak suggesting the presence of large soluble molecule that is very stable (Figure 12).

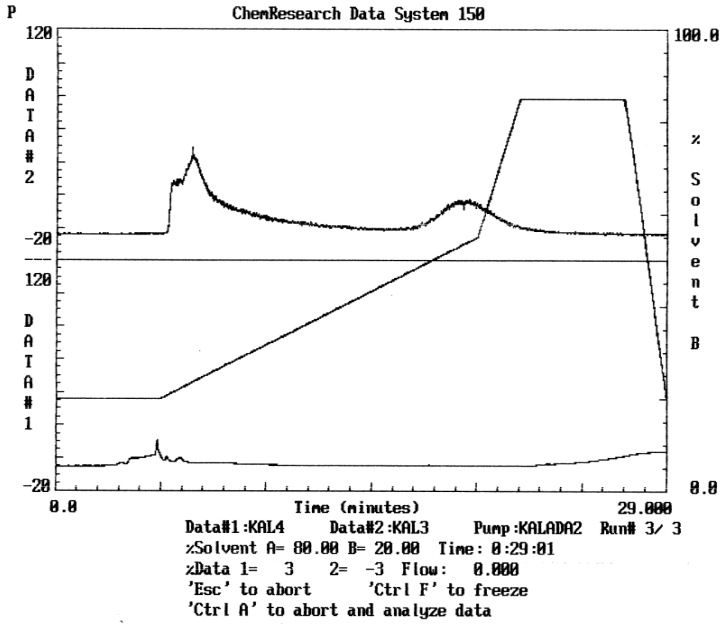

**Figure 12. Kalata B1-G3-C12 stability.** Compound stability was tested in vitro by incubating $^{111}$In-DOTA radiolabeled test compounds in mouse serum for 14 h. Radiolabeling was performed at 60° for 1 h. Sample characterized by reversed phase HPLC analysis. Each chromatogram traces the simultaneous measurements of radioactivity on top and absorbance at 280 nm on the bottom.

In Figure 13, the ability of the radiolabeled cyclotide to bind gal-3-expressing breast cancer cells was evaluated. As shown, the kalata B1-G3-C12 construct bound well to the MDA-MB-435 cancer cells but not to BT549 gal-3 negative cells.

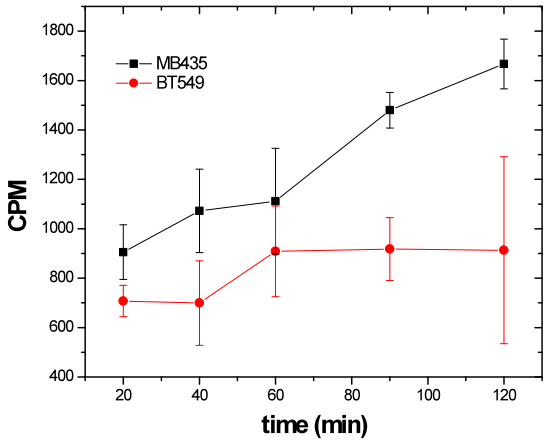


**Figure 13. Kalata B1-G3-C12 Binding.** 50,000 cpm of $^{111}$In-DOTA radiolabeled compound was incubated with gal-3-positive (MDA-MB-435) and negative (BT549) human breast cancer cells at 37˚C for different times. After incubation, the media was aspirated and the cells were rinsed and centrifuged. The radioactivity bound to the cells was counted.

The Kalata B1-G3-C12 cyclotide was also labeled with $^{68}$Ga via a NOTA bifunctional chelator. The labeling and cell binding of the scaffold is shown in Figure 14.

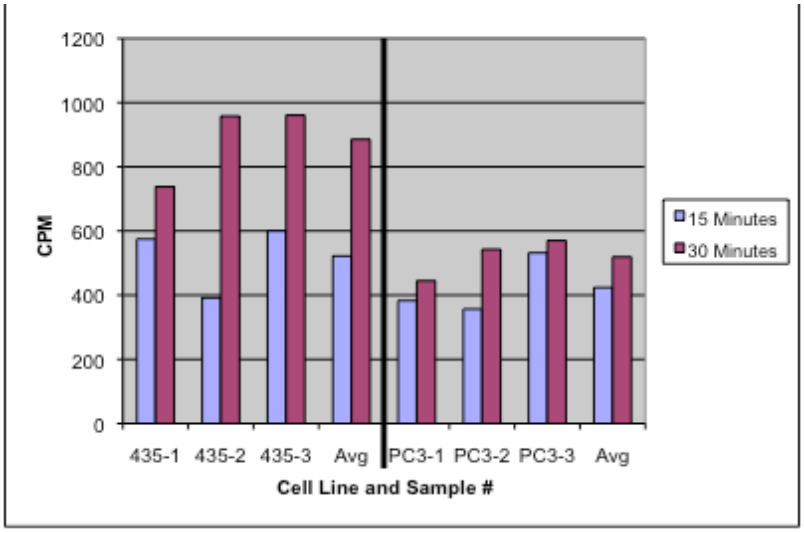


**Figure 14. Labeling G3-C12 with $^{68}$Ga and Cell Binding**. The peptide cyclotide was labeled with $^{68}$Ga eluted from a Ge-68 generator with 0.1M HCl, and added to 0.5 mg of DOTA peptide in 0.5 mL of 0.5M ammonium acetate, pH 5. The reaction was incubated at 80°C for 7 minutes and free $^{68}$Ga was removed. Radiochemical purity was 90% and radiolabeled peptide was

analyzed for cancer cell specificity and affinity by cell binding to MDA-MB-435 breast cancer cells (gal-3-positive) and PC3 cells (gal-3-negative).

**3. In Vivo PET/optical imaging of gal-3/carbohydrate interactions using radio- and fluorescently- labeled peptide conjugates.** For biodistributions, we labeled the cyclotides that target gal-3 and TF with $^{111}$In, because of difficulty in large scale purification of $^{68}$Ga cyclotides. Radiomaging studies were not successful (very little in vivo tumor uptake) but optical imaging studies demonstrated some uptake.

The gal-3-targeting G3-C12 peptide in the form of a cyclotide loop scaffold (Kalata B1-G3-C12) was radiolabeled with $^{111}$In and its biodistribution properties compared to the linear peptide (Figure 15).

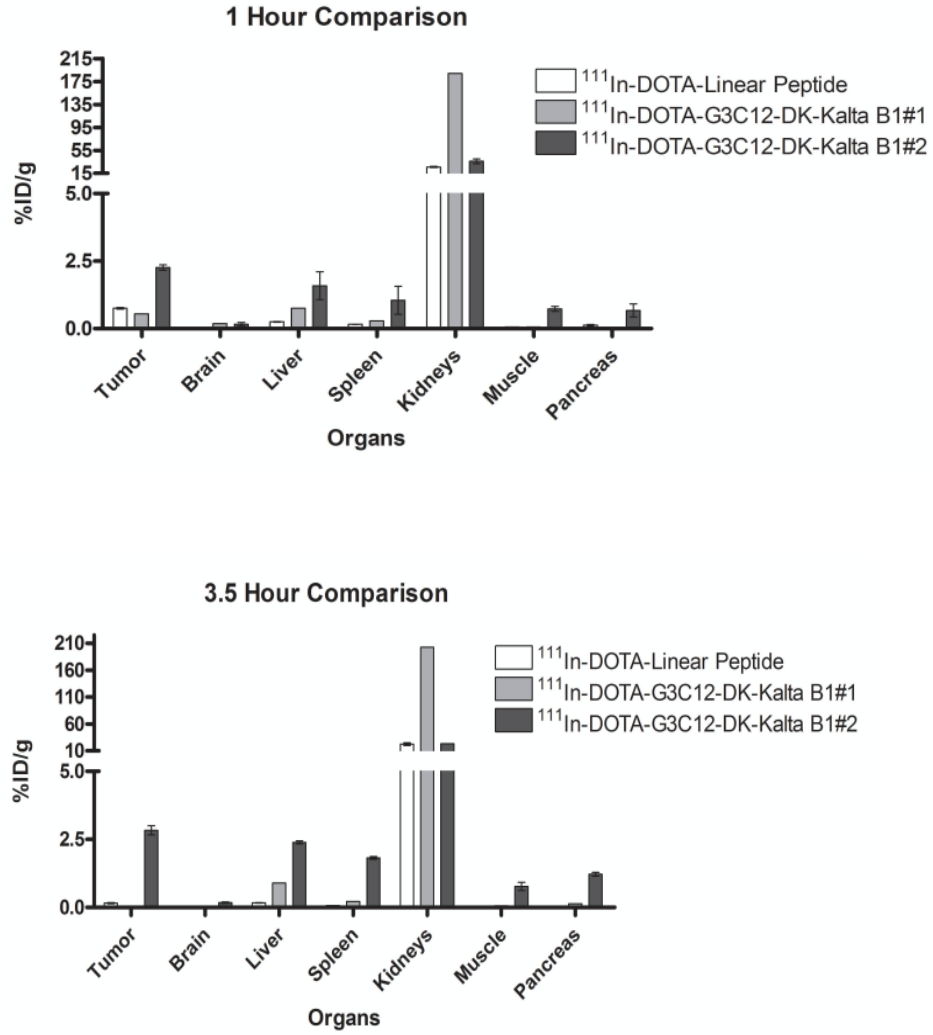


**Figure 15. Biodistribution of Kalata B1-G3-C12 in SCID bearing MDA-MB-435 human breast carcinoma.** Kalata B1-G3-C12 was folded as previously described. 36 μM of Kalata B1 in 600 μM acetic acid, at pH 3.5, was mixed with 0.5 uCi of $^{111}$InCl and incubated at 42°C for 1 hour. The labeled compound was purified via RP-HPLC.

The results of these studies show very high renal binding. At one hour, the renal binding of the 3- and 4-disulfide compounds peaks at 30% and 40% respectively. The tumor binding is seen as 1% for three-disulfide and 2.3% four-disulfide compounds at 1 hour. For each compound the

tumor binding results are significantly above binding seen in liver, spleen, muscle and pancreas. At 3.5 hours, the renal accumulation is not changed much with 30% ID/g for each compound. The total tumor accumulation for the four-disulfide compound has risen to 2.8% while the three-disulfide compound has dropped to 0.25%, an almost 10-fold difference between the two. It should be noted that although the four-disulfide compound continues to show significantly higher tumor accumulation than spleen, muscle and pancreas, it is only slightly more significant than the activity measured in the liver. It was found that the $^{111}$In-DOTA-G3C12-DK-KalataB1#2 (with four disulfide bonds) was superior to KalataB1#1 (three disulfides) and linear G3-C12 in terms of tumor uptake. $^{111}$In-DOTA-G3C12-DK-KalataB1#1 had high kidney uptake. Thus, $^{111}$In-DOTA-G3C12-DK-KalataB1#2 will be used in future in vivo imaging.

Both gal-3 and TF –targeting peptides were fluorescently labeled (ASF680) and examined as peptide scaffolds for in vivo optical imaging. Shown below is fluorescent TF-peptide/scaffold uptake in animals xenografted with TF-expressing tumors (Figure 16).

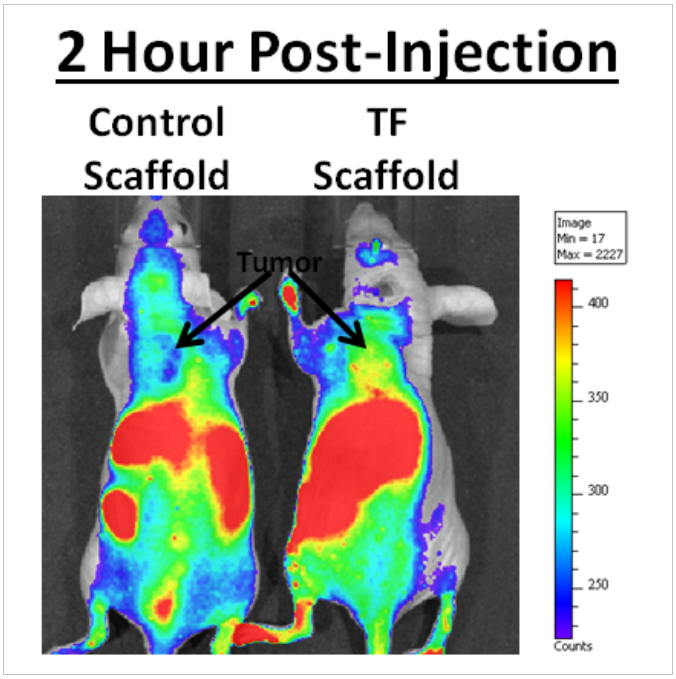

**Figure 16. Optical Imaging of TF-expressing Cells.** Scaffolds labeled with AlexaFluor680 (AF680) were intravenously injected into tumor bearing mice and allowed to circulate for 2 hours. Anesthetized mice were imaged at 2 hours post-injection.

We have shown that we can synthesize gal-3 binding epitopes into loop 6 of the cyclotide Kalata B1 with biotin, DOTA and NOTA chelating groups. The peptides can be cyclized, purified, and refolded while retaining their binding affinity. The radiolabeled peptides are acceptably stable in vitro. Biodistribution studies in vivo indicate the cyclotide containing the full length G3-C12 Gal-3 binding peptide has a serum stability half-life compared to the linear peptide while having an improved tumor uptake. A longer experimental endpoint may show improved tumor uptake versus non-target organ uptake. While, PET imaging did not show significant uptake, optical imaging of the constructs demonstrated tumor uptake in gal-3 and TF- expressing cells.